



HAL
open science

Higher order interface conditions for piezoelectric spherical hollow composites: asymptotic approach and transfer matrix homogenization method

Michele Serpilli, Raffaella Rizzoni, Serge Dumont, Frédéric Lebon

► To cite this version:

Michele Serpilli, Raffaella Rizzoni, Serge Dumont, Frédéric Lebon. Higher order interface conditions for piezoelectric spherical hollow composites: asymptotic approach and transfer matrix homogenization method. *Composite Structures*, 2022, 279, pp.114760. 10.1016/j.compstruct.2021.114760 . hal-03546056

HAL Id: hal-03546056

<https://hal.science/hal-03546056>

Submitted on 30 Apr 2024

HAL is a multi-disciplinary open access archive for the deposit and dissemination of scientific research documents, whether they are published or not. The documents may come from teaching and research institutions in France or abroad, or from public or private research centers.

L'archive ouverte pluridisciplinaire **HAL**, est destinée au dépôt et à la diffusion de documents scientifiques de niveau recherche, publiés ou non, émanant des établissements d'enseignement et de recherche français ou étrangers, des laboratoires publics ou privés.

Higher order interface conditions for piezoelectric spherical hollow composites: asymptotic approach and transfer matrix homogenization method

M. Serpilli^{a,*}, R. Rizzoni^b, S. Dumont^c, F. Lebon^d

^a *Department of Civil and Building Engineering, and Architecture, Università Politecnica delle Marche, Ancona, Italy*

^b *Department of Engineering, University of Ferrara, Ferrara, Italy*

^c *IMAG CNRS UMR 5149, University of Nîmes, Nîmes, France*

^d *Aix-Marseille Univ, CNRS, Centrale Marseille, LMA, Marseille, France*

The paper describes the mechanical behavior of composites made of piezoelectric spheres in perfect or imperfect contact. The imperfect contact is achieved by interposing piezoelectric thin adhesive layers between the spheres. First, using asymptotic analysis, transmission conditions of imperfect interface equivalent to the behavior of piezoelectric adhesive layers are obtained at order 0 and 1. These transmission conditions are calculated for "hard" adhesives, i.e. adhesive materials whose electromechanical constants do not rescale with their thickness. Next, under the assumption of spherical symmetry, the transmission conditions are condensed to a general law of imperfect contact, able to simultaneously describe different contact regimes: piezoelectric hard (order 0 and 1) and soft (or spring-type, order 0 and 1) interface conditions, the perfect continuity conditions, and the piezoelectric rigid (Gurtin–Murdoch or membrane-type) conditions. Lastly, following Bifulco's approach, the homogenization problem of a spherical hollow piezoelectric assembly is solved, extending the classical transfer matrix method to take into account the presence of thin adhesive layers described using the proposed transmission conditions of imperfect contact. A simple numerical example is provided, illustrating the correctness and effectiveness of the homogenization approach in describing the electromechanical behavior of spherical piezoelectric assemblies.

1. Introduction

Piezoelectric materials have been extensively employed in the design of smart structures, active control, sensors and actuators, thanks to their ability to exchange electrical inputs to mechanical deformation, and, conversely, to transform a mechanical action into an electric potential. They can be used in small members for electromechanical devices as well as structural components in disks, cylindrical and spherical shells in several engineering applications such as energy harvesting [1], hydroacoustics [2], health monitoring [3], and transducers [4]. Moreover, in order to control the distribution of the main physical quantities, piezoelectric structures can be made of several layers, which can be suitably stacked or glued together forming a laminated composite with desired effective electromechanical properties [5]. For this particular structures, it is important to develop an exact solution relating the applied loads to displacement, stresses and electric potential. A vast literature on radial spherical piezoelectric transducers has been reported. Many researches analyzed the electromechanical behavior of

piezoelectric hollow spheres, developing analytical solutions for stress and electric potential fields, e.g. [6–8], taking into account pyroelectric effects and thermal gradients [9–11]. The electromechanical analysis have also been extended to functionally graded materials [12], coated sensors [13] and sandwich assemblies [14].

Concerning the theoretical analysis of bonded joints, the thin interphase layer between to adjacent media can be treated as a two-dimensional surface, called the imperfect interface, on which appropriate transmission conditions are defined. Various interface models have been developed throughout the years by means of classical variational tools and more refined mathematical techniques (asymptotic analysis), spanning from uncoupled phenomena, such as thermal conduction [15–17] and elasticity [18–23], to multifield and multiphysics theories [24,25], such as continua with microstructure [26,27], coupled thermoelasticity [28] and piezoelectricity [29,30].

The present paper aims at providing a general form of the interface law for piezoelectric spherical hollow composites by means of

* Corresponding author.

E-mail address: m.serpilli@univpm.it (M. Serpilli).

an asymptotic analysis. The piezoelectric assembly is constituted by the inner and outer adherents, connected together by an intermediate radial bonded joint, whose thickness depends on a small parameter ϵ . The material coefficients of the piezoelectric constituents are assumed independent of ϵ . This allows to characterize the so-called hard interface model. Following the asymptotic approaches developed in [24,31], it is possible to compute the interface law at order 0, corresponding to classical continuity conditions, and the order 1 transmission conditions, defining a non trivial interface model. The above conditions have been specialized in the case of spherical radial symmetry. Combining the results at order 0 and order 1, a general interface model has been obtained, which comprises in itself the soft (spring-type), hard and rigid (Gurtin–Murdoch or membrane-type) interface laws, as shown in [24].

Various homogenization procedures for layered media have been developed throughout the years, based on the determination of the composite effective constitutive coefficients. In the present paper, the transfer matrix method by Buefler [32,33] is taken into consideration. A similar homogenization technique for the derivation of an effective average model of periodic media has been developed by Molotkov in [34], with applications to the propagation of seismic and acoustic waves. The aforementioned homogenization methods are basically equivalent, since they rely on a particular formulation of the governing equations as a first-order linear system in terms of the state vector Fourier's transform (containing displacements and stresses). Even though the system solution is expressed with two different representations, namely, with an exponential matrix in [32], and through the successive approximation method in [34], the final results can be considered analogous. Besides, Molotkov provided a multiphysic and multifield generalization of the homogenization method, applied to Biot's poroelastic layered continua (see [35]).

In this work, a generalization of the transfer matrix method [32,33] is proposed for piezoelectric hollow spherical composites. Moreover, the aforementioned general interface laws have been implemented within the homogenization procedure, allowing to define equivalent elastic material parameters. Lastly, a numerical example has been developed considering a simple three-layer piezoelectric composite, subjected to an assigned electric potential on the inner boundary. The exact solution of the three-layer configuration is compared with the closed-form solution of a two-layer composite, in which the intermediate adhesive has been replaced by the general interface conditions. Besides, a third comparison has been made taking into account the single-layer homogenized solution obtained through the transfer matrix method.

2. Asymptotic analysis in terms of spherical coordinates

2.1. The governing equations of the problem

Let us consider an orthonormal spherical basis $(\mathbf{e}_r, \mathbf{e}_\theta, \mathbf{e}_\varphi)$, denoting the three curvilinear coordinates of a point of the body. The equilibrium equations for a deformable body and the electrostatics charge equation (in the absence of volume forces and free charge density) in spherical coordinates are respectively defined as follows (see [7,9]) :

$$\begin{aligned} \sigma_{rr,r} + \frac{1}{r \sin \varphi} \sigma_{r\theta,\theta} + \frac{1}{r} \sigma_{r\varphi,\varphi} + \frac{1}{r} (2\sigma_{rr} - \sigma_{\theta\theta} - \sigma_{\varphi\varphi} + \sigma_{r\varphi} \cot \varphi) &= 0, \\ \sigma_{r\varphi,r} + \frac{1}{r \sin \varphi} \sigma_{\theta\varphi,\theta} + \frac{1}{r} \sigma_{\varphi\varphi,\varphi} + \frac{1}{r} (3\sigma_{r\varphi} + (\sigma_{\varphi\varphi} - \sigma_{\theta\theta}) \cot \varphi) &= 0, \\ \sigma_{r\theta,r} + \frac{1}{r \sin \varphi} \sigma_{\theta\theta,\theta} + \frac{1}{r} \sigma_{\theta\varphi,\varphi} + \frac{1}{r} (3\sigma_{r\theta} + 2\sigma_{\theta\varphi} \cot \varphi) &= 0, \\ D_{r,r} + \frac{1}{r} D_{\varphi,\varphi} + \frac{1}{r \sin \varphi} D_{\theta,\theta} + \frac{2}{r} D_r + \frac{2 \cot \varphi}{r} D_\varphi &= 0, \end{aligned} \quad (1)$$

where $\sigma = (\sigma_{ij})$ and $\mathbf{D} = (D_i)$, $i, j = r, \theta, \varphi$, represent, respectively, the spherical components of the Cauchy stress tensor and electric

displacement field. The constitutive law for a spherically transversely isotropic piezoelectric material takes the following form:

$$\begin{aligned} \sigma_{rr} &= c_{11} \epsilon_{rr} + c_{12} \epsilon_{\theta\theta} + c_{12} \epsilon_{\varphi\varphi} - e_{11} E_r, \\ \sigma_{\theta\theta} &= c_{12} \epsilon_{rr} + c_{22} \epsilon_{\theta\theta} + c_{23} \epsilon_{\varphi\varphi} - e_{12} E_r, \\ \sigma_{\varphi\varphi} &= c_{12} \epsilon_{rr} + c_{23} \epsilon_{\theta\theta} + c_{22} \epsilon_{\varphi\varphi} - e_{12} E_r, \\ \sigma_{r\varphi} &= 2c_{44} \epsilon_{r\varphi} - e_{15} E_\varphi, \\ \sigma_{r\theta} &= 2c_{44} \epsilon_{r\theta} - e_{15} E_\theta, \\ \sigma_{\theta\varphi} &= (c_{22} - c_{23}) \epsilon_{\theta\varphi}, \\ D_r &= e_{11} \epsilon_{rr} + e_{12} \epsilon_{\theta\theta} + e_{12} \epsilon_{\varphi\varphi} + \beta_{11} E_r, \\ D_\varphi &= 2e_{15} \epsilon_{r\varphi} + \beta_{22} E_\varphi, \\ D_\theta &= 2e_{15} \epsilon_{r\theta} + \beta_{22} E_\theta, \end{aligned} \quad (2)$$

where c_{ij} , e_{ij} and β_{ij} denote the elastic, piezoelectric and electric conductivity coefficients and $\epsilon = (\epsilon_{ij})$ and $\mathbf{E} = (E_i)$ represent, respectively, the spherical components of the linearized strain tensor and electric field, which can be expressed in the terms of the spherical coordinates through the following relations:

$$\begin{aligned} \epsilon_{rr} &= u_{r,r}, \\ \epsilon_{\varphi\varphi} &= \frac{1}{r} u_{\varphi,\varphi} + \frac{1}{r} u_r, \\ \epsilon_{\theta\theta} &= \frac{1}{r \sin \varphi} u_{\theta,\theta} + \frac{\cot \varphi}{r} u_\varphi + \frac{1}{r} u_r, \\ \epsilon_{r\varphi} &= \frac{1}{r} u_{r,\varphi} + u_{\varphi,r} - \frac{1}{r} u_\varphi, \\ \epsilon_{\varphi\theta} &= \frac{1}{r \sin \varphi} u_{\varphi,\theta} + \frac{1}{r} u_{\theta,\varphi} - \frac{\cot \varphi}{r} u_\theta, \\ \epsilon_{r\theta} &= \frac{1}{r \sin \varphi} u_{r,\theta} + u_{\theta,r} - \frac{1}{r} u_\theta, \\ E_r &= -\phi_{,r}, \\ E_\varphi &= -\frac{1}{r} \phi_{,\varphi}, \\ E_\theta &= -\frac{1}{r \sin \varphi} \phi_{,\theta}, \end{aligned} \quad (3)$$

with u_r , u_φ , u_θ , the radial, azimuthal and circumferential components of the displacement field along the basis $(\mathbf{e}_r, \mathbf{e}_\theta, \mathbf{e}_\varphi)$, and ϕ , the electric potential.

2.2. The interface conditions for a radial bonded joint

The spherical piezoelectric hollow assembly is constituted by the inner and outer adherents Ω_+^ϵ and Ω_-^ϵ , connected by a intermediate adhesive layer B^ϵ . The gluing between the two adherents is assumed along the radial direction. The thickness of the adhesive is supposed to be constant and equal to ϵ . The bonded joint lies in the interval $(r_0 - \epsilon/2, r_0 + \epsilon/2)$. To apply the asymptotic expansions method, a change of variables is needed, in order to rewrite the governing equations of a fixed domain (independent of ϵ), see Fig. 1. The change of variable is introduced along the radial direction:

$$\begin{aligned} (\hat{r}, \hat{\theta}, \hat{\varphi}) &:= \hat{\pi}(r, \theta, \varphi) = (r_0 + \frac{r-r_0}{\epsilon}, \theta, \varphi) \text{ in } B^\epsilon, \\ (\bar{r}, \bar{\theta}, \bar{\varphi}) &:= \bar{\pi}(r, \theta, \varphi) = (r, \theta, \varphi) \pm \left(\frac{\epsilon}{2} \mp \frac{1}{2} \right) \mathbf{e}_r \text{ in } \Omega_\pm^\epsilon. \end{aligned}$$

In the sequel, $R := r_0 + \frac{r-r_0}{\epsilon}$. The rescaled domains will be noted with B and Ω_\pm . Moreover, only if necessary, \hat{g} and \bar{g} will denote, respectively, the restrictions of function g to B and Ω_\pm .

The change of variables implies that

$$\partial_R = \frac{1}{\epsilon} \partial_r, \quad \text{and} \quad \frac{1}{r} = \frac{1}{r_0 + \epsilon(R - r_0)} = \frac{1}{r_0} - \frac{R - r_0}{r_0^2} \epsilon + o(\epsilon).$$

The constitutive coefficients of the adherents and adhesive are assumed to be independent of ϵ . Since the rescaled problem on a fixed domain present a polynomial structure with respect to the small parameter ϵ , we can look for the solution of the problem as a series of powers of ϵ ,

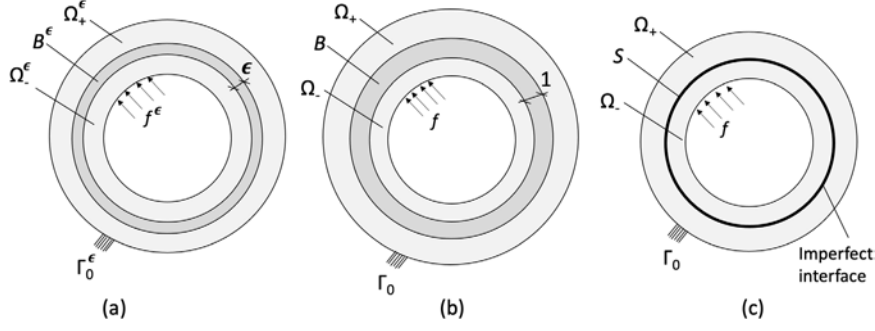


Fig. 1. Initial (a), rescaled (b) and limit (c) configurations of the spherical composite.

as follows:

$$\begin{aligned}
 \boldsymbol{\sigma}^\epsilon &= \boldsymbol{\sigma}^0 + \epsilon \boldsymbol{\sigma}^1 + \epsilon^2 \boldsymbol{\sigma}^2 + \dots, \\
 \mathbf{u}^\epsilon &= \mathbf{u}^0 + \epsilon \mathbf{u}^1 + \epsilon^2 \mathbf{u}^2 + \dots, \\
 \mathbf{D}^\epsilon &= \mathbf{D}^0 + \epsilon \mathbf{D}^1 + \epsilon^2 \mathbf{D}^2 + \dots, \\
 \phi^\epsilon &= \phi^0 + \epsilon \phi^1 + \epsilon^2 \phi^2 + \dots.
 \end{aligned} \tag{4}$$

By applying the change of variables to the governing Eqs. (1) and by substituting the asymptotic expansions (4), one has:

$$\begin{aligned}
 &\frac{1}{\epsilon} \sigma_{rr,R}^0 + \sigma_{rr,R}^1 + \frac{1}{r_0 \sin \varphi} \sigma_{r\theta,\theta}^0 + \frac{1}{r_0} \sigma_{r\varphi,\varphi}^0 \\
 &\quad + \frac{1}{r_0} (2\sigma_{rr}^0 - \sigma_{\theta\theta}^0 - \sigma_{\varphi\varphi}^0 + \sigma_{r\varphi}^0 \cot \varphi) + \dots = 0, \\
 &\frac{1}{\epsilon} \sigma_{r\varphi,R}^0 + \sigma_{r\varphi,R}^1 + \frac{1}{r_0 \sin \varphi} \sigma_{\theta\varphi,\theta}^0 + \frac{1}{r_0} \sigma_{\varphi\varphi,\varphi}^0 \\
 &\quad + \frac{1}{r_0} (3\sigma_{r\varphi}^0 + (\sigma_{\varphi\varphi}^0 - \sigma_{\theta\theta}^0) \cot \varphi) + \dots = 0, \\
 &\frac{1}{\epsilon} \sigma_{r\theta,R}^0 + \sigma_{r\theta,R}^1 + \frac{1}{r_0 \sin \varphi} \sigma_{\theta\theta,\theta}^0 + \frac{1}{r_0} \sigma_{\theta\varphi,\varphi}^0 \\
 &\quad + \frac{1}{r_0} (3\sigma_{r\theta}^0 + 2\sigma_{\theta\varphi}^0 \cot \varphi) + \dots = 0, \\
 &\frac{1}{\epsilon} D_{r,R}^0 + D_{r,R}^1 + \frac{1}{r_0} D_{\varphi,\varphi}^0 + \frac{1}{r_0 \sin \varphi} D_{\theta,\theta}^0 \\
 &\quad + \frac{2}{r_0} D_r^0 + \frac{2 \cot \varphi}{r_0} D_\varphi^0 + \dots = 0.
 \end{aligned} \tag{5}$$

The same procedure is considered for the strain tensor and electric field components (3). Thus,

$$\begin{aligned}
 \epsilon_{rr}^\epsilon &= \frac{1}{\epsilon} u_{r,R}^0 + u_{r,R}^1 + \dots, \\
 \epsilon_{\varphi\varphi}^\epsilon &= \frac{1}{r_0} u_{\varphi,\varphi}^0 + \frac{1}{r_0} u_r^0 + \dots, \\
 \epsilon_{\theta\theta}^\epsilon &= \frac{1}{r_0 \sin \varphi} u_{\theta,\theta}^0 + \frac{\cot \varphi}{r_0} u_\varphi^0 + \frac{1}{r} u_r^0 + \dots, \\
 \epsilon_{r\varphi}^\epsilon &= \frac{1}{\epsilon} u_{\varphi,R}^0 + u_{\varphi,R}^1 + \frac{1}{r_0} u_{r,\varphi}^0 - \frac{1}{r_0} u_\varphi^0 + \dots, \\
 \epsilon_{\varphi\theta}^\epsilon &= \frac{1}{r_0 \sin \varphi} u_{\theta,\theta}^0 + \frac{1}{r_0} u_{\theta,\varphi}^0 - \frac{\cot \varphi}{r_0} u_\theta^0 + \dots, \\
 \epsilon_{r\theta}^\epsilon &= \frac{1}{\epsilon} u_{\theta,R}^0 + u_{\theta,R}^1 + \frac{1}{r_0 \sin \varphi} u_{r,\theta}^0 - \frac{1}{r_0} u_\theta^0 + \dots, \\
 E_r^\epsilon &= -\frac{1}{\epsilon} \phi_{,R}^0 - \phi_{,R}^1 + \dots, \\
 E_\varphi^\epsilon &= -\frac{1}{r_0} \phi_{,\varphi}^0 + \dots, \\
 E_\theta^\epsilon &= -\frac{1}{r_0 \sin \varphi} \phi_{,\theta}^0 + \dots.
 \end{aligned}$$

By injecting the above rescaled strains and electric field into the constitutive relations (2), we obtain:

$$\begin{aligned}
 \sigma_{rr}^0 + \dots &= \frac{1}{\epsilon} (c_{11} u_{r,R}^0 + e_{11} \phi_{,R}^0) + \left\{ c_{12} \left(\frac{1}{r_0 \sin \varphi} u_{\theta,\theta}^0 + \frac{\cot \varphi}{r_0} u_\varphi^0 + \frac{1}{r} u_r^0 \right) + \right. \\
 &\quad \left. + c_{12} \left(\frac{1}{r_0} u_{\varphi,\varphi}^0 + \frac{1}{r_0} u_r^0 \right) + c_{11} u_{r,R}^1 + e_{11} \phi_{,R}^1 \right\} + \dots, \\
 \sigma_{\theta\theta}^0 + \dots &= \frac{1}{\epsilon} (c_{12} u_{r,R}^0 + e_{12} \phi_{,R}^0) + \left\{ c_{22} \left(\frac{1}{r_0 \sin \varphi} u_{\theta,\theta}^0 + \frac{\cot \varphi}{r_0} u_\varphi^0 + \frac{1}{r} u_r^0 \right) + \right. \\
 &\quad \left. + c_{23} \left(\frac{1}{r_0} u_{\varphi,\varphi}^0 + \frac{1}{r_0} u_r^0 \right) + c_{12} u_{r,R}^1 + e_{12} \phi_{,R}^1 \right\} + \dots, \\
 \sigma_{\varphi\varphi}^0 + \dots &= \frac{1}{\epsilon} (c_{12} u_{r,R}^0 + e_{12} \phi_{,R}^0) + \left\{ c_{23} \left(\frac{1}{r_0 \sin \varphi} u_{\theta,\theta}^0 + \frac{\cot \varphi}{r_0} u_\varphi^0 + \frac{1}{r} u_r^0 \right) + \right. \\
 &\quad \left. + c_{22} \left(\frac{1}{r_0} u_{\varphi,\varphi}^0 + \frac{1}{r_0} u_r^0 \right) + c_{12} u_{r,R}^1 + e_{12} \phi_{,R}^1 \right\} + \dots, \\
 \sigma_{r\varphi}^0 + \dots &= \frac{1}{\epsilon} 2c_{44} u_{\varphi,R}^0 + 2c_{44} \left(u_{\varphi,R}^1 + \frac{1}{r_0} u_{r,\varphi}^0 - \frac{1}{r_0} u_\varphi^0 \right) + \frac{e_{15}}{r_0} \phi_{,\varphi}^0 + \dots, \\
 \sigma_{r\theta}^0 + \dots &= \frac{1}{\epsilon} 2c_{44} u_{\theta,R}^0 + 2c_{44} \left(u_{\theta,R}^1 + \frac{1}{r_0 \sin \varphi} u_{r,\theta}^0 - \frac{1}{r_0} u_\theta^0 \right) + \frac{e_{15}}{r_0 \sin \varphi} \phi_{,\theta}^0 + \dots, \\
 \sigma_{\theta\varphi}^0 + \dots &= (c_{22} - c_{23}) \left(\frac{1}{r_0 \sin \varphi} u_{\theta,\theta}^0 + \frac{1}{r_0} u_{\theta,\varphi}^0 - \frac{\cot \varphi}{r_0} u_\theta^0 \right) + \dots, \\
 D_r^0 + \dots &= \frac{1}{\epsilon} (e_{11} u_{r,R}^0 - \beta_{11} \phi_{,R}^0) + \left\{ e_{12} \left(\frac{1}{r_0 \sin \varphi} u_{\theta,\theta}^0 + \frac{\cot \varphi}{r_0} u_\varphi^0 + \frac{1}{r} u_r^0 \right) + \right. \\
 &\quad \left. + e_{12} \left(\frac{1}{r_0} u_{\varphi,\varphi}^0 + \frac{1}{r_0} u_r^0 \right) + e_{11} u_{r,R}^1 - \beta_{11} \phi_{,R}^1 \right\} + \dots, \\
 D_\varphi^0 + \dots &= \frac{1}{\epsilon} 2e_{15} u_{\varphi,R}^0 + 2e_{15} \left(u_{\varphi,R}^1 + \frac{1}{r_0} u_{r,\varphi}^0 - \frac{1}{r_0} u_\varphi^0 \right) - \frac{\beta_{22}}{r_0} \phi_{,\varphi}^0 + \dots, \\
 D_\theta^0 + \dots &= \frac{1}{\epsilon} 2e_{15} u_{\theta,R}^0 + 2e_{15} \left(u_{\theta,R}^1 + \frac{1}{r_0 \sin \varphi} u_{r,\theta}^0 - \frac{1}{r_0} u_\theta^0 \right) - \frac{\beta_{22}}{r_0 \sin \varphi} \phi_{,\theta}^0 + \dots.
 \end{aligned} \tag{6}$$

The interface conditions at order 0 and order 1 can be characterized by identifying the terms with identical power of ϵ . Focusing on the terms occurring in ϵ^{-1} in Eq. (5), we get:

$$\sigma_{rr,R}^0 = 0, \quad \sigma_{r\varphi,R}^0 = 0, \quad \sigma_{r\theta,R}^0 = 0, \quad D_{r,R}^0 = 0,$$

which imply that σ_{rr}^0 , $\sigma_{r\varphi}^0$, $\sigma_{r\theta}^0$ and D_r^0 are constant with respect to the radial coordinate R . Due to the continuity of the radial traction vector and electric displacement at the interface between adherends and adhesive, their jumps, evaluated at $R = \pm \frac{1}{2}$, vanish, i.e. $[\sigma_{rr}^0] = 0$, $[\sigma_{r\varphi}^0] = 0$, $[\sigma_{r\theta}^0] = 0$ and $[D_r^0] = 0$, where $[\cdot]$ denotes the jump functions. Moreover, $\langle \sigma_{rr}^0 \rangle = \sigma_{rr}^0$, $\langle \sigma_{r\varphi}^0 \rangle = \sigma_{r\varphi}^0$, $\langle \sigma_{r\theta}^0 \rangle = \sigma_{r\theta}^0$ and $\langle D_r^0 \rangle = D_r^0$, with $\langle \cdot \rangle$ denotes the mean value.

Considering relations (6)_{1,7,4,5} at order -1 , one has:

$$c_{11} u_{r,R}^0 + e_{11} \phi_{,R}^0 = 0, \quad e_{11} u_{r,R}^0 - \beta_{11} \phi_{,R}^0 = 0, \quad u_{\varphi,R}^0 = 0, \quad u_{\theta,R}^0 = 0.$$

The solution of the above linear system implies that the displacement field, u_r^0 , u_φ^0 , u_θ^0 , and the electric potential ϕ^0 , at order 0, are constant along the radial direction. By virtue of the continuity conditions at the interface level between the inner and outer spheres and the adhesive layer, the following jumps $[u_r^0] = 0$, $[u_\varphi^0] = 0$, $[u_\theta^0] = 0$ and $[\phi^0] = 0$

are equal to zero. As customary, $\langle u_r^0 \rangle = u_r^0$, $\langle u_\varphi^0 \rangle = u_\varphi^0$, $\langle u_\theta^0 \rangle = u_\theta^0$ and $\langle \phi^0 \rangle = \phi^0$.

In view of the above, the interface transmission conditions at order 0 shows a perfect interface model, equivalent to the classical continuity conditions:

$$\begin{aligned} [\sigma_{rr}^0] &= 0, & [\sigma_{r\varphi}^0] &= 0, & [\sigma_{r\theta}^0] &= 0, & [D_r^0] &= 0, \\ [u_r^0] &= 0, & [u_\varphi^0] &= 0, & [u_\theta^0] &= 0, & [\phi^0] &= 0. \end{aligned}$$

Let us consider Eqs. (6)_{1,7,4,5} at order 0 and isolate the terms related to the displacements and electric potential at order 1:

$$\begin{aligned} c_{11}u_{r,R}^1 + e_{11}\phi_{,R}^1 &= \sigma_{rr}^0 - c_{12}(\varepsilon_{\varphi\varphi}^0 + \varepsilon_{\theta\theta}^0), \\ e_{11}u_{r,R}^1 - \beta_{11}\phi_{,R}^1 &= D_r^0 - e_{12}(\varepsilon_{\varphi\varphi}^0 + \varepsilon_{\theta\theta}^0), \\ u_{\varphi,R}^1 &= \sigma_{r\varphi}^0 - \varepsilon_{r\varphi}^0 - \frac{e_{15}}{2c_{44}} \frac{1}{r_0} \phi_{,\varphi}^0, \\ u_{\theta,R}^1 &= \sigma_{r\theta}^0 - \varepsilon_{r\theta}^0 - \frac{e_{15}}{2c_{44}} \frac{1}{r_0 \sin \varphi} \phi_{,\theta}^0. \end{aligned} \quad (7)$$

with $\varepsilon_{\varphi\varphi}^0 := \frac{1}{r_0} u_{\varphi,\varphi}^0 + \frac{1}{r_0} u_r^0$, $\varepsilon_{\theta\theta}^0 := \frac{1}{r_0 \sin \varphi} u_{\theta,\theta}^0 + \frac{\cot \varphi}{r_0} u_\varphi^0 + \frac{1}{r} u_r^0$, $\varepsilon_{r\varphi}^0 := \frac{1}{r_0} u_{r,\varphi}^0 - \frac{1}{r_0} u_\varphi^0$ and $\varepsilon_{r\theta}^0 := \frac{1}{r_0 \sin \varphi} u_{r,\theta}^0 - \frac{1}{r_0} u_\theta^0$, depending only on the terms at order 0. After an integration along the radial coordinate $R = r_0 \pm \frac{1}{2}$, the solution of the previous linear system allows to characterize the jump of the displacement field and electric potential at order 1, as follows:

$$\begin{aligned} [u_r^1] &= \frac{1}{c_{11}\beta_{11} + e_{11}^2} \left\{ \beta_{11}\sigma_{rr}^0 + e_{11}D_r^0 + (\beta_{11}c_{12} + e_{11}e_{12})(\varepsilon_{\varphi\varphi}^0 + \varepsilon_{\theta\theta}^0) \right\}, \\ [\phi^1] &= \frac{1}{c_{11}\beta_{11} + e_{11}^2} \left\{ e_{11}\sigma_{rr}^0 - c_{11}D_r^0 - (c_{12}e_{11} - c_{11}e_{12})(\varepsilon_{\varphi\varphi}^0 + \varepsilon_{\theta\theta}^0) \right\}, \\ [u_\varphi^1] &= \sigma_{r\varphi}^0 - \varepsilon_{r\varphi}^0 - \frac{e_{15}}{2c_{44}} \frac{1}{r_0} \phi_{,\varphi}^0, \\ [u_\theta^1] &= \sigma_{r\theta}^0 - \varepsilon_{r\theta}^0 - \frac{e_{15}}{2c_{44}} \frac{1}{r_0 \sin \varphi} \phi_{,\theta}^0. \end{aligned} \quad (8)$$

Moreover, the obtained values of $u_{r,R}^1$, $u_{\varphi,R}^1$, $u_{\theta,R}^1$ and $\phi_{,R}^1$ can be helpful to derive explicit expressions of $\sigma_{\varphi\varphi}^0$, $\sigma_{\theta\theta}^0$, $\sigma_{\theta\varphi}^0$, D_φ^0 and D_θ^0 as functions of the zeroth order terms.

The equilibrium and electrostatic charge equations at order 0 give:

$$\begin{aligned} \sigma_{rr,R}^1 &= -\frac{1}{r_0 \sin \varphi} \sigma_{r\theta,\theta}^0 - \frac{1}{r_0} \sigma_{r\varphi,\varphi}^0 - \frac{1}{r_0} \left(2\sigma_{rr}^0 - \sigma_{\theta\theta}^0 - \sigma_{\varphi\varphi}^0 + \sigma_{r\varphi}^0 \cot \varphi \right), \\ \sigma_{r\varphi,R}^1 &= -\frac{1}{r_0 \sin \varphi} \sigma_{\theta\varphi,\theta}^0 - \frac{1}{r_0} \sigma_{\varphi\varphi,\varphi}^0 - \frac{1}{r_0} \left(3\sigma_{r\varphi}^0 + (\sigma_{\varphi\varphi}^0 - \sigma_{\theta\theta}^0) \cot \varphi \right), \\ \sigma_{r\theta,R}^1 &= -\frac{1}{r_0 \sin \varphi} \sigma_{\theta\theta,\theta}^0 - \frac{1}{r_0} \sigma_{\theta\varphi,\varphi}^0 - \frac{1}{r_0} \left(3\sigma_{r\theta}^0 + 2\sigma_{\theta\varphi}^0 \cot \varphi \right), \\ D_{r,R}^1 &= -\frac{1}{r_0} D_{\varphi,\varphi}^0 - \frac{1}{r_0 \sin \varphi} D_{\theta,\theta}^0 - \frac{2}{r_0} D_r^0 - \frac{2 \cot \varphi}{r_0} D_\varphi^0. \end{aligned}$$

By integrating the previous equations along the radial direction and by applying the continuity conditions of the radial traction vector and radial electric displacement, one can formulate the final interface conditions at order 1:

$$\begin{aligned} [\sigma_{rr}^1] &= -\frac{1}{r_0 \sin \varphi} \sigma_{r\theta,\theta}^0 - \frac{1}{r_0} \sigma_{r\varphi,\varphi}^0 - \\ &\quad - \frac{1}{r_0} \left\{ 2 \left(1 - \frac{2(\beta_{11}c_{12} + e_{11}e_{12})}{c_{11}\beta_{11} + e_{11}^2} \right) \sigma_{rr}^0 - \frac{2(c_{12}e_{11} - c_{11}e_{12})}{c_{11}\beta_{11} + e_{11}^2} D_r^0 - \right. \\ &\quad \left. - \left(c_{22} + c_{23} + \frac{2c_{12}(\beta_{11}c_{12} + e_{11}e_{12}) - 2e_{12}(c_{12}e_{11} - c_{11}e_{12})}{c_{11}\beta_{11} + e_{11}^2} \right) (\varepsilon_{\varphi\varphi}^0 + \varepsilon_{\theta\theta}^0) \right\}, \\ [\sigma_{r\varphi}^1] &= -\frac{1}{r_0 \sin \varphi} (c_{22} - c_{23}) \varepsilon_{\theta\varphi,\theta}^0 - \frac{1}{r_0} \left\{ 3\sigma_{r\varphi}^0 + (c_{23} - c_{22})(\varepsilon_{\varphi\varphi}^0 + \varepsilon_{\theta\theta}^0) \cot \varphi \right\} - \\ &\quad - \frac{1}{r_0} \left\{ \frac{\beta_{11}c_{12} + e_{11}e_{12}}{c_{11}\beta_{11} + e_{11}^2} \sigma_{rr,\varphi}^0 + \frac{c_{12}e_{11} - c_{11}e_{12}}{c_{11}\beta_{11} + e_{11}^2} D_{r,\varphi}^0 + \right. \\ &\quad \left. + \left(c_{22} + \frac{c_{12}(\beta_{11}c_{12} + e_{11}e_{12}) - e_{12}(c_{12}e_{11} - c_{11}e_{12})}{c_{11}\beta_{11} + e_{11}^2} \right) \varepsilon_{\theta\theta,\varphi}^0 + \right. \\ &\quad \left. + \left(c_{23} + \frac{c_{12}(\beta_{11}c_{12} + e_{11}e_{12}) - e_{12}(c_{12}e_{11} - c_{11}e_{12})}{c_{11}\beta_{11} + e_{11}^2} \right) \varepsilon_{\varphi\varphi,\varphi}^0 \right\}, \\ [\sigma_{r\theta}^1] &= -\frac{1}{r_0} (c_{22} - c_{23}) \varepsilon_{\theta\varphi,\theta}^0 - \frac{1}{r_0} \left\{ 3\sigma_{r\theta}^0 + 2(c_{22} - c_{23}) \varepsilon_{\theta\varphi}^0 \cot \varphi \right\} - \\ &\quad - \frac{1}{r_0 \sin \varphi} \left\{ \frac{\beta_{11}c_{12} + e_{11}e_{12}}{c_{11}\beta_{11} + e_{11}^2} \sigma_{rr,\theta}^0 + \frac{c_{12}e_{11} - c_{11}e_{12}}{c_{11}\beta_{11} + e_{11}^2} D_{r,\theta}^0 + \right. \\ &\quad \left. + \left(c_{23} + \frac{c_{12}(\beta_{11}c_{12} + e_{11}e_{12}) - e_{12}(c_{12}e_{11} - c_{11}e_{12})}{c_{11}\beta_{11} + e_{11}^2} \right) \varepsilon_{\theta\theta,\theta}^0 + \right. \\ &\quad \left. + \left(c_{22} + \frac{c_{12}(\beta_{11}c_{12} + e_{11}e_{12}) - e_{12}(c_{12}e_{11} - c_{11}e_{12})}{c_{11}\beta_{11} + e_{11}^2} \right) \varepsilon_{\varphi\varphi,\theta}^0 \right\}, \\ [D_r^1] &= -\frac{2D_r^0}{r_0} - \frac{1}{r_0} \left\{ 2e_{15}\sigma_{r\varphi,\varphi}^0 - \frac{1}{r_0} \frac{e_{15}^2 + \beta_{22}c_{44}}{c_{44}} \phi_{,\varphi\varphi}^0 \right\} - \\ &\quad - \frac{1}{r_0} \left\{ 2e_{15}\sigma_{r\theta,\theta}^0 - \frac{1}{r_0 \sin \varphi} \frac{e_{15}^2 + \beta_{22}c_{44}}{c_{44}} \phi_{,\theta\theta}^0 \right\} - \\ &\quad - \frac{\cot \varphi}{r_0} \left\{ 2e_{15}\sigma_{r\varphi}^0 - \frac{1}{r_0} \frac{e_{15}^2 + \beta_{22}c_{44}}{c_{44}} \phi_{,\varphi}^0 \right\}. \end{aligned} \quad (9)$$

Eqs. (8) and (9) represent the higher order interface laws for a piezoelectric spherical composite. These conditions provide the simultaneous jumps of the displacement field, electric potential, stress field and electric displacement at order 1 depending on the values of the same physical quantities at order 0. These order 0 terms are known since they have been determined in the previous problem and they appear in the formulation as source terms. The interface conditions at order 1 can be interpreted as the two-dimensional piezoelectric equilibrium problem defined on the plane of the interface.

2.3. The interface conditions for a radial bonded joint: spherical symmetry

In the case of a spherically symmetric problem, radially polarized, radially transversely isotropic hollow spherical composite, the radial displacement field and electric potential depend only on the radial coordinate, i.e., $u_r^\varepsilon = u_r^\varepsilon(r)$, $\phi^\varepsilon = \phi^\varepsilon(r)$, while both the circumferential and azimuthal displacements vanish, i.e. $u_\varphi^\varepsilon = u_\theta^\varepsilon = 0$. By virtue of the symmetry assumptions, the equilibrium and electrostatic problems simplify since the only non null stresses and electric displacements are $\sigma_{rr}^\varepsilon = \sigma_{rr}^\varepsilon(r)$ and $D_r^\varepsilon = D_r^\varepsilon(r)$. Interface conditions at order 0 maintain the same form:

$$[u_r^0] = 0, \quad [\phi^0] = 0, \quad [\sigma_{rr}^0] = 0, \quad [D_r^0] = 0, \quad (10)$$

while the interface conditions at order 1 reduces to:

$$\begin{aligned} [u_r^1] &= \frac{1}{c_{11}\beta_{11} + e_{11}^2} \left\{ \beta_{11}\sigma_{rr}^0 + e_{11}D_r^0 - 2(\beta_{11}c_{12} + e_{11}e_{12}) \frac{u_r^0}{r_0} \right\}, \\ [\phi^1] &= \frac{1}{c_{11}\beta_{11} + e_{11}^2} \left\{ e_{11}\sigma_{rr}^0 - c_{11}D_r^0 + 2(c_{12}e_{11} - c_{11}e_{12}) \frac{u_r^0}{r_0} \right\}, \\ [\sigma_{rr}^1] &= \frac{2}{r_0} \left\{ \left(\frac{\beta_{11}c_{12} + e_{11}e_{12}}{c_{11}\beta_{11} + e_{11}^2} - 1 \right) \sigma_{rr}^0 + \frac{c_{12}e_{11} - c_{11}e_{12}}{c_{11}\beta_{11} + e_{11}^2} D_r^0 + \right. \end{aligned}$$

$$[D_r^1] = -\frac{2}{r_0} D_r^0 + \left(c_{22} + c_{23} - \frac{2c_{12}(\beta_{11}c_{12} + e_{11}e_{12}) + 2e_{12}(c_{12}e_{11} - c_{11}e_{12})}{c_{11}\beta_{11} + e_{11}^2} \right) \frac{u_r^0}{r_0} \Bigg\}, \quad (11)$$

The above transmission conditions represent a piezoelectric generalization of the interface law, obtained in [31], in the case of an elastic spherical laminated composite.

In [24], it has been shown that it is possible to obtain a condensed form of transmission conditions (10)–(11), summarizing both the orders 0 and 1, and defining an implicit general piezoelectric interface law. To this end, by denoting by $\tilde{u}_r^\epsilon := u_r^0 + \epsilon u_r^1$, $\tilde{\sigma}_{rr}^\epsilon := \sigma_{rr}^0 + \epsilon \sigma_{rr}^1$, $\tilde{D}_r^\epsilon := D_r^0 + \epsilon D_r^1$ and $\tilde{\phi}^\epsilon := \phi^0 + \epsilon \phi^1$, suitable approximations of u_r^ϵ , σ_{rr}^ϵ , D_r^ϵ , and ϕ^ϵ respectively, one can obtain an equivalent implicit form of the transmission conditions:

$$\begin{aligned} \langle \tilde{\sigma}_{rr}^\epsilon \rangle &= \tilde{c}_{11}^\epsilon \frac{[\tilde{u}_r^\epsilon]}{\epsilon} + \tilde{e}_{11}^\epsilon \frac{[\tilde{\phi}^\epsilon]}{\epsilon} + 2\tilde{e}_{12}^\epsilon \frac{[\tilde{u}_r^\epsilon]}{r_0} \\ \langle \tilde{D}_r^\epsilon \rangle &= \tilde{e}_{11}^\epsilon \frac{[\tilde{u}_r^\epsilon]}{\epsilon} - \tilde{\beta}_{11}^\epsilon \frac{[\tilde{\phi}^\epsilon]}{\epsilon} + 2\tilde{e}_{12}^\epsilon \frac{[\tilde{u}_r^\epsilon]}{r_0} \\ [\tilde{\sigma}_{rr}^\epsilon] &= 2(\tilde{c}_{12}^\epsilon - \tilde{c}_{11}^\epsilon) \frac{[\tilde{u}_r^\epsilon]}{r_0} + 2(\tilde{e}_{12}^\epsilon - \tilde{e}_{11}^\epsilon) \frac{[\tilde{\phi}^\epsilon]}{r_0} + 2(\tilde{c}_{22}^\epsilon - \tilde{c}_{23}^\epsilon - 2\tilde{c}_{12}^\epsilon) \frac{\epsilon \langle \tilde{u}_r^\epsilon \rangle}{r_0^2}, \\ [\tilde{D}_r^\epsilon] &= -2\tilde{e}_{11}^\epsilon \frac{[\tilde{u}_r^\epsilon]}{r_0} + 2\tilde{\beta}_{11}^\epsilon \frac{[\tilde{\phi}^\epsilon]}{r_0} - 4\tilde{e}_{12}^\epsilon \frac{\epsilon \langle \tilde{u}_r^\epsilon \rangle}{r_0^2}. \end{aligned} \quad (12)$$

With arguments similar to those used in [24], where a flat adhesive was considered, it can be shown that the above relations comprise three different contact regimes at various orders (order 0 and 1), namely the piezoelectric soft (or spring-type) interface conditions, the perfect continuity conditions, and the piezoelectric rigid (Gurtin–Murdoch or membrane-type) conditions, and are expected to provide a better approximation of the behavior of the thin curved interphase.

3. Transfer matrix method

In this section, a spherical hollow assembly model, consisting of N different, radially polarized, transversely isotropic thin layers, is studied using the transfer matrix method. The transfer matrix method is a classical approach [32,33]. Here, we first review its application to a piezoelectric hollow sphere, then we generalize the technique to an arbitrarily laminated piezoelectric hollow sphere and, finally, we extend the obtained results to the case of imperfect contact between the layers, with a general interface law comprising the order 0 and order 1 transmission conditions obtained in Section 2.2.

3.1. The piezoelectric hollow sphere

The basic equilibrium and electrostatic charge equations in the case of spherical symmetric loading read (see [7]):

$$\begin{aligned} \sigma_{r,r} + \frac{2}{r}(\sigma_{rr} + \sigma_{\theta\theta}) &= 0, \\ D_{r,r} + \frac{2}{r}D_r &= 0, \end{aligned} \quad (13)$$

while the constitutive equations for radially polarized and transversely isotropic piezoelectric material are:

$$\begin{aligned} \sigma_{rr} &= c_{11}u_{r,r} + 2c_{12}\frac{u_r}{r} + e_{11}\phi_{,r}, \\ \sigma_{\theta\theta} &= c_{12}u_{r,r} + (c_{22} + c_{23})\frac{u_r}{r} + e_{12}\phi_{,r}, \\ D_r &= e_{11}u_{r,r} + 2e_{12}\frac{u_r}{r} - \beta_{11}\phi_{,r}. \end{aligned} \quad (14)$$

Following the approach by [33], it is possible to express the governing equations, combined with the constitutive laws, as follows:

$$a_{,r}(r) = \mathbf{A}(r)\mathbf{a}(r) \quad (15)$$

with

$$\mathbf{A}(r) := \begin{bmatrix} \frac{A_{11}}{r} & \frac{A_{12}}{r^2} & \frac{A_{13}}{r} & 0 \\ A_{21} & \frac{A_{22}}{r} & A_{23} & 0 \\ 0 & 0 & \frac{A_{33}}{r} & 0 \\ A_{41} & \frac{A_{42}}{r} & A_{43} & 0 \end{bmatrix}, \quad \mathbf{a}(r) := \begin{bmatrix} \sigma_{rr}(r) \\ u_r(r) \\ D_r(r) \\ \phi(r) \end{bmatrix}, \quad (16)$$

and

$$\begin{aligned} A_{11} &:= 2 \left(\frac{\beta_{11}c_{12} + e_{11}e_{12}}{c_{11}\beta_{11} + e_{11}^2} - 1 \right), \quad A_{13} := \frac{2(c_{12}e_{11} - c_{11}e_{12})}{c_{11}\beta_{11} + e_{11}^2}, \\ A_{12} &:= 2 \left(c_{22} + c_{23} - \frac{2c_{12}(\beta_{11}c_{12} + e_{11}e_{12}) + 2e_{12}(c_{12}e_{11} - c_{11}e_{12})}{c_{11}\beta_{11} + e_{11}^2} \right), \\ A_{21} &:= \frac{\beta_{11}}{c_{11}\beta_{11} + e_{11}^2}, \quad A_{22} := -\frac{2(\beta_{11}c_{12} + e_{11}e_{12})}{c_{11}\beta_{11} + e_{11}^2}, \quad A_{23} := \frac{e_{11}}{c_{11}\beta_{11} + e_{11}^2}, \\ A_{33} &:= -2, \quad A_{41} := \frac{e_{11}}{c_{11}\beta_{11} + e_{11}^2}, \quad A_{42} := \frac{2(c_{11}e_{12} - e_{11}c_{12})}{c_{11}\beta_{11} + e_{11}^2}, \\ A_{43} &:= -\frac{c_{11}}{c_{11}\beta_{11} + e_{11}^2}, \end{aligned} \quad (17)$$

with the compatibility condition $A_{11} + A_{22} = -2$. Matrix $\mathbf{A}(r)$ is called the fundamental matrix and $\mathbf{a}(r)$ the state vector. In the sequel, we recall the general solution of the equilibrium and electrostatic problems for a piezoelectric hollow sphere, free of volume forces and charge density, developed in [7] and adapted for the purposes of the present work:

$$\begin{aligned} \sigma_{rr}(r) &= a_{11}F_1r^{\alpha_1-1} + a_{12}F_2r^{\alpha_2-1} + a_{13}F_3\frac{1}{r^2}, \\ u_r(r) &= F_1r^{\alpha_1} + F_2r^{\alpha_2} + F_3a_{23}\frac{1}{r}, \\ D_r(r) &= F_3\frac{1}{r^2}, \\ \phi(r) &= a_{41}F_1r^{\alpha_1} + a_{42}F_2r^{\alpha_2} + a_{43}F_3\frac{1}{r} + F_4, \end{aligned} \quad (18)$$

where $\alpha_{1/2} := \frac{1}{2}(-1 \pm \sqrt{1 + 8\beta})$, $2\beta = A_{12}A_{21} + (1 + A_{22})A_{22}$, and

$$\begin{aligned} a_{11} &:= \frac{\alpha_1 - A_{22}}{A_{21}}, \quad a_{12} := \frac{\alpha_2 - A_{22}}{A_{21}}, \\ a_{13} &:= -\frac{a_{23}(1 + A_{22}) + A_{23}}{A_{21}}, \\ a_{23} &:= \frac{1}{2\beta} (A_{23}(2 + A_{11}) - A_{21}A_{13}), \\ a_{41} &:= \frac{1}{\alpha_1} (A_{41}a_{11} + A_{42}), \quad a_{42} := \frac{1}{\alpha_2} (A_{41}a_{12} + A_{42}), \\ a_{43} &:= -(A_{43} + A_{41}a_{13} + A_{42}a_{23}). \end{aligned}$$

The previous coefficients are analogous to those obtained in [7], see Appendix. F_1 , F_2 , F_3 and F_4 represent the integration constants, that can be found applying a proper set of mechanical and electrical boundary conditions. The solution can be rewritten in matrix form:

$$\begin{bmatrix} \sigma_{rr}(r) \\ u_r(r) \\ D_r(r) \\ \phi(r) \end{bmatrix} = \begin{bmatrix} a_{11}r^{\alpha_1-1} & a_{12}r^{\alpha_2-1} & \frac{a_{13}}{r^2} & 0 \\ r^{\alpha_1} & r^{\alpha_2} & \frac{a_{23}}{r} & 0 \\ 0 & 0 & \frac{1}{r^2} & 0 \\ a_{41}r^{\alpha_1} & a_{42}r^{\alpha_2} & \frac{a_{43}}{r} & 1 \end{bmatrix} \begin{bmatrix} F_1 \\ F_2 \\ F_3 \\ F_4 \end{bmatrix}$$

In compact form, $\mathbf{a}(r) = \mathbf{B}(r)\mathbf{F}$. Having in mind the transfer-matrix method, we replace the integration constants F_1 , F_2 , F_3 and F_4 by the initial state variables $\sigma_{rr}(r_0)$, $u_r(r_0)$, $D_r(r_0)$ and $\phi(r_0)$, i.e. $\mathbf{a}(r_0)$. As customary, the integration constants vector can be obtained through $\mathbf{F} = \mathbf{B}^{-1}(r_0)\mathbf{a}(r_0)$ and, thus,

$$\mathbf{a}(r) = \mathbf{T}(r)\mathbf{a}(r_0), \quad (19)$$

where $\mathbf{T}(r) := \mathbf{B}(r)\mathbf{B}^{-1}(r_0)$ is the field-transfer matrix from radius r_0 to radius r , which has the following expression

$$\mathbf{T}(r) := \frac{1}{a_{11} - a_{12}} \begin{bmatrix} T_{11}(r) & T_{12}(r) & T_{13}(r) & 0 \\ T_{21}(r) & T_{22}(r) & T_{23}(r) & 0 \\ 0 & 0 & T_{33}(r) & 0 \\ T_{41}(r) & T_{42}(r) & T_{43}(r) & 1 \end{bmatrix},$$

with

$$\begin{aligned} T_{11}(r) &:= a_{11} \left(\frac{r}{r_0}\right)^{\alpha_1-1} - a_{12} \left(\frac{r}{r_0}\right)^{\alpha_2-1}, \\ T_{12}(r) &:= -\frac{a_{11}a_{12}}{r_0} \left\{ \left(\frac{r}{r_0}\right)^{\alpha_1-1} - \left(\frac{r}{r_0}\right)^{\alpha_2-1} \right\}, \\ T_{13}(r) &:= \frac{(a_{11} - a_{12})a_{13}}{\left(\frac{r}{r_0}\right)^2} + a_{11}(a_{12}a_{23} - a_{13}) \left(\frac{r}{r_0}\right)^{\alpha_1-1} \\ &\quad + a_{12}(a_{13} - a_{11}a_{23}) \left(\frac{r}{r_0}\right)^{\alpha_2-1}, \\ T_{21}(r) &:= r_0 \left\{ \left(\frac{r}{r_0}\right)^{\alpha_1} - \left(\frac{r}{r_0}\right)^{\alpha_2} \right\}, \\ T_{22}(r) &:= a_{11} \left(\frac{r}{r_0}\right)^{\alpha_2} - a_{12} \left(\frac{r}{r_0}\right)^{\alpha_1}, \\ T_{23}(r) &:= \frac{(a_{11} - a_{12})a_{23}r_0}{\left(\frac{r}{r_0}\right)^2} + r_0(a_{12}a_{23} - a_{13}) \left(\frac{r}{r_0}\right)^{\alpha_1} \\ &\quad + r_0(a_{13} - a_{11}a_{23}) \left(\frac{r}{r_0}\right)^{\alpha_2}, \\ T_{41}(r) &:= a_{42} \left(1 - \left(\frac{r}{r_0}\right)^{\alpha_2}\right) - a_{41} \left(1 - \left(\frac{r}{r_0}\right)^{\alpha_1}\right), \\ T_{42}(r) &:= a_{12}a_{41} \left(1 - \left(\frac{r}{r_0}\right)^{\alpha_1}\right) - a_{11}a_{42} \left(1 - \left(\frac{r}{r_0}\right)^{\alpha_2}\right), \\ T_{43}(r) &:= \frac{(a_{11} - a_{12})a_{43}r_0}{\frac{r}{r_0}} + r_0a_{41}(a_{12}a_{23} - a_{13}) \left(\frac{r}{r_0}\right)^{\alpha_1} \\ &\quad + r_0a_{42}(a_{13} - a_{11}a_{23}) \left(\frac{r}{r_0}\right)^{\alpha_2} \\ &\quad + r_0(a_{13}(a_{41}a_{42}) + a_{43}(a_{12} - a_{11}) + a_{23}(a_{11}a_{42} - a_{12}a_{41})). \end{aligned}$$

Note that the field-transfer matrix $\mathbf{T}(r)$ and the fundamental matrix $\mathbf{A}(r)$ are related to each other according to the relation: $\mathbf{A}(r_0) = \mathbf{T}_{,r}(r)|_{r=r_0}$.

3.2. The laminated piezoelectric hollow sphere

Let us consider a laminated piezoelectric hollow sphere, constituted by N layers. Each layer (k) is characterized by the corresponding material parameters, marked by the index k , and the radii r_{k-1} and r_k , and thickness $h_k := r_k - r_{k-1}$. A dimensionless coordinate ρ for the layer (k) is defined according to

$$\rho = \frac{r - r_{k-1}}{r_{k-1}}, \quad r_{k-1} \leq r \leq r_k, \quad \rho_k = \frac{h_k}{r_{k-1}}, \quad \frac{r}{r_{k-1}} = 1 + \rho.$$

The transfer equation (19), with $r_0 = r_{k-1}$, can be rewritten as follows:

$$\mathbf{a}^{(k)}(\rho) = \mathbf{T}^{(k)}(\rho)\mathbf{a}^{(k)}(0),$$

where $\mathbf{T}^{(k)}(\rho)$ is the transfer matrix of layer (k). The states at both boundaries of layer (k) are connected by

$$\mathbf{a}^{(k)}(\rho_k) = \mathbf{T}^{(k)}(\rho_k)\mathbf{a}^{(k)}(0),$$

and, by means of the continuity conditions, $\mathbf{a}^{(k)}(0) = \mathbf{a}^{(k-1)}(\rho_{k-1}) := \mathbf{a}_{k-1}$, $k = 1, \dots, N-1$, one has:

$$\mathbf{a}_k = \mathbf{T}_k \mathbf{a}_{k-1}, \quad (20)$$

where $\mathbf{T}_k := \mathbf{T}^{(k)}(\rho_k)$ represents the layer-transfer matrix of layer (k) from radius r_{k-1} to r_k . Applying (20) N -times for the layered hollow sphere made of layers in perfect contact, we get

$$\mathbf{a}_N = \mathbf{S}\mathbf{a}_0, \quad \mathbf{S} := \mathbf{T}_N \mathbf{T}_{N-1} \dots \mathbf{T}_1.$$

Here \mathbf{S} denote the system-transfer matrix from radius r_0 to radius r_N , because it connects the state vectors at the boundaries of the laminated hollow sphere. Knowing the initial state vector \mathbf{a}_0 on the internal boundary, it is possible to find the state vector in each layer.

Let us suppose that $h_k = \lambda_k h$, where $h := \sum_{k=1}^N h_k$ is the total thickness of the laminated hollow sphere and $0 < \lambda_k < 1$ is a thickness ratio, satisfying $\sum_{k=1}^N \lambda_k = 1$. The assumption of small thickness of each layer h_k with respect to r_0 , so that $h_k \ll r_0$, implies that

$$\rho_k = \frac{h_k}{r_{k-1}} = \frac{\lambda_k h}{r_0 + h \sum_{i=1}^{k-1} \lambda_i} = \frac{\lambda_k h}{r_0} + o(h^2),$$

and, hence, the layer-transfer matrix \mathbf{T}_k admits the following representation:

$$\mathbf{T}_k = \mathbf{I} - h\lambda_k \mathbf{M}_k + o(h^2),$$

where the elements of matrix \mathbf{M}_k coincides with the elements of matrix $-\mathbf{A}(r_0)$ (cf. (16)), corresponding to k th layer. As a consequence, the system-transfer matrix \mathbf{S} presents an analogous asymptotic development:

$$\mathbf{S} = \mathbf{I} - h\mathbb{M} + o(h^2), \quad (21)$$

where $\mathbb{M} := \sum_{k=1}^N \lambda_k \mathbf{M}_k$.

3.3. The laminated piezoelectric hollow sphere with imperfect interface conditions

In the previous section, the problem of a laminated piezoelectric hollow sphere with perfect contact has been analyzed. In order to extend these results to a laminated sphere with imperfect contact between the layers, ad hoc transmission conditions must be considered at the spherical surface between adjacent layers (see [31]).

Assume that the thickness of each interface layer $\epsilon_k = \xi_k h$, with $\xi_k \ll 1$, $k = 1, \dots, N-1$. In order to apply the Bifuler's approach, it is necessary to define an interface transfer matrix between radii $r_k := r_k^-$ and $r_k + \epsilon_k := r_k^+$. Substituting the explicit forms of the jump $[\cdot]$ and mean value $\langle \cdot \rangle$ into (12), the interface conditions can be rewritten as follows, with self-explanatory notation:

$$\mathbf{a}_k^+ = \hat{\mathbf{K}}_k \mathbf{a}_k^-, \quad \mathbf{a}_k^- := \mathbf{a}^{(k)}(\rho_k), \quad \mathbf{a}_k^+ := \mathbf{a}^{(k)}(\rho_k + \epsilon_k/r_{k-1}),$$

where \mathbf{a}_k^+ and \mathbf{a}_k^- represent the state vectors at the top and bottom interfaces, respectively, and

$$\hat{\mathbf{K}}_k := \mathbf{I} - h\xi_k \hat{\mathbf{N}}_k + o(h^2).$$

It can be shown that the coefficients of matrix $\hat{\mathbf{N}}_k$ surprisingly coincides with the elements of $-\mathbf{A}(r_0)$ (cf. (16)), in which the interface material parameters are considered. Now, thanks to the presence of the imperfect interface, the system-transfer matrix system $\tilde{\mathbf{S}}$ (cf. (21)) modifies in order to incorporate the matrices $\hat{\mathbf{K}}_k$:

$$\tilde{\mathbf{S}} = \mathbf{T}_N \hat{\mathbf{K}}_{N-1} \mathbf{T}_{N-1} \dots \hat{\mathbf{K}}_1 \mathbf{T}_1 = \mathbf{I} - h\mathbb{L} + o(h^2),$$

where $\mathbb{L} := \sum_{k=1}^N \lambda_k \mathbf{M}_k + \sum_{\ell=1}^{N-1} \xi_\ell \hat{\mathbf{N}}_\ell$. Following Bifuler [33], the system matrix for the hollow sphere with homogenized properties is calculated as

$$\mathbf{a}_{,r} = \lim_{h \rightarrow 0} \frac{\tilde{\mathbf{S}} - \mathbf{I}}{h} \mathbf{a}_0 = -\mathbb{L} \mathbf{a}_0,$$

and, thus, choosing $r = r_0$,

$$\mathbf{a}_{,r}(r) = \langle \mathbf{A}(r) \rangle \mathbf{a}(r), \quad \langle \mathbf{A}(r) \rangle := \begin{bmatrix} \frac{\langle A_{11} \rangle}{r} & \frac{\langle A_{12} \rangle}{r^2} & \frac{\langle A_{13} \rangle}{r} & 0 \\ \langle A_{21} \rangle & \frac{\langle A_{22} \rangle}{r} & \langle A_{23} \rangle & 0 \\ 0 & 0 & \frac{\langle A_{33} \rangle}{r} & 0 \\ \langle A_{41} \rangle & \frac{\langle A_{42} \rangle}{r} & \langle A_{43} \rangle & 0 \end{bmatrix}, \quad (22)$$

where $\langle \mathbf{A}(r) \rangle$ denotes the fundamental matrix of the homogenized laminated piezoelectric hollow sphere, such that $\langle \mathbf{A}(r_0) \rangle = -\mathbb{L}$. Indeed,

by comparing (22) with (15) for a piezoelectric homogeneous hollow sphere, we notice that the governing equations are analogous but with different coefficients. The coefficients of the fundamental matrix $\langle \mathbf{A}(r) \rangle$ for a laminated hollow sphere, comprising also the presence of the general imperfect interface law, reduce to the sum of $\langle \mathbf{A}(r) \rangle$ coefficients for each adherent and interface layer, taking into account their thickness ratios, namely λ_k and ξ_{ℓ} , respectively. Indeed, one has

$$\langle A_{ij} \rangle := \sum_{k=1}^N \lambda_k A_{ij}^{(k)} + \sum_{\ell=1}^{N-1} \xi_{\ell} \hat{A}_{ij}^{(\ell)},$$

where $A_{ij}^{(k)}$ and $\hat{A}_{ij}^{(\ell)}$ represent, respectively, coefficients (16) relative to the k -th layer and the ℓ -th interface layer. It is worth-mentioning that the use of the general imperfect contact laws, described in (12), corresponds to the actual insertion of a thin spherical interphase layer between adjacent adherents. Hence, the problem of an arbitrarily laminated piezoelectric hollow sphere is equivalent to the problem of an homogenized one.

Remark. The case of a periodic laminated piezoelectric hollow sphere, made of a layer group of n generally different basic layers, can be easily obtained by choosing $h_k = \frac{\lambda_k h}{n}$ and $\epsilon_k = \frac{\xi_k h}{n}$. In this case, the fundamental matrix satisfies $\langle \mathbf{A}(r_0) \rangle = -n\mathbb{I}$.

As an example let us consider the simple case of a spherical composite, made of two adherents and an intermediate interface layer. Thus, the system matrix $\tilde{\mathbf{S}} = \mathbf{T}^+ \hat{\mathbf{K}} \mathbf{T}^-$, with \mathbf{T}^{\pm} , the transfer matrices of the top and bottom spheres, and $\hat{\mathbf{K}}$, the interface transfer matrix. The adherents thickness ratios are chosen as $\lambda_k^+ = \lambda_k^- = \frac{1}{2}$, while the adhesive thickness ratio is ξ . Note that comparing the present results with the fundamental matrices of a transversely isotropic homogeneous elastic sphere (cf. [33], eqns. (17)–(19)), one obtains the equivalent elastic material parameters $\frac{E}{1-\nu}$, $\frac{1}{\nu'}$ and $\frac{\nu'}{E'}$ of the homogenized piezoelectric spherical composite, where E , E' , ν and $\nu' = \nu \frac{E'}{E}$ denote, respectively, the radial and tangential stiffness moduli, and the major and minor Poisson's coefficients. These material parameters depend on the piezoelectric moduli, defined in the constitutive equation (14), and can be thought as equivalent elastic engineering constants for the composite. The result is

$$\begin{aligned} \frac{E}{1-\nu} &= \frac{1}{2} \langle A_{12} \rangle = \frac{1}{2} \frac{\Delta^+}{c_{11}^+ \beta_{11}^+ + (e_{11}^+)^2} + \frac{1}{2} \frac{\Delta^-}{c_{11}^- \beta_{11}^- + (e_{11}^-)^2} + \xi \frac{\hat{\Delta}}{\hat{c}_{11} \hat{\beta}_{11} + \hat{e}_{11}^2}, \\ \frac{\nu'}{E'} &= -\frac{\langle A_{22} \rangle}{\langle A_{12} \rangle} = \frac{1}{2} \frac{\beta_{11}^+ e_{12}^+ + e_{11}^+ e_{12}^+}{\Delta^+} + \frac{1}{2} \frac{\beta_{11}^- e_{12}^- + e_{11}^- e_{12}^-}{\Delta^-} + \xi \frac{\hat{\beta}_{11} \hat{e}_{12} + \hat{e}_{11} \hat{e}_{12}}{\hat{\Delta}}, \\ \frac{1}{E'} &= \frac{\langle A_{22} \rangle^2}{\langle A_{12} \rangle} + \langle A_{21} \rangle = \frac{1}{2(c_{11}^+ \beta_{11}^+ + (e_{11}^+)^2)} \left(\frac{(\beta_{11}^+ e_{12}^+ + e_{11}^+ e_{12}^+)^2}{\Delta^+} + \beta_{11}^+ \right) + \\ &+ \frac{1}{2(c_{11}^- \beta_{11}^- + (e_{11}^-)^2)} \left(\frac{\beta_{11}^- e_{12}^- + e_{11}^- e_{12}^-}{\Delta^-} + \beta_{11}^- \right) \\ &+ \frac{\xi}{\hat{c}_{11} \hat{\beta}_{11} + \hat{e}_{11}^2} \left(\frac{\hat{\beta}_{11} \hat{e}_{12} + \hat{e}_{11} \hat{e}_{12}}{\hat{\Delta}} + \hat{\beta}_{11} \right). \end{aligned} \quad (23)$$

with $\Delta := (c_{22} + c_{23})(c_{11} \beta_{11} + e_{11}^2) - 2c_{12}(\beta_{11} c_{12} + e_{11} e_{12}) + 2e_{12}(c_{12} e_{11} - c_{11} e_{12})$.

4. A simple numerical example

Let us consider a three-layer hollow piezoelectric sphere with inner radius $r_0 = 10$ cm, see Fig. 2. The internal and external layers are 0.5 cm thick, while the thickness of the intermediate adhesive layer depends on a small parameter ϵ , such that $\epsilon \ll 0.5$ cm. Let us denote with $r_1^- = 10.5$ cm, $r_1^+ = 10.5 + \epsilon$ cm and $r_2 = 11 + \epsilon$ cm, the values of the radii referred to inner and outer interfaces between the adherents and adhesive, and the outer radius, respectively. The total thickness h of the layered sphere is equal to $r_2 - r_0 = 1 + \epsilon$ cm. The adherents are constituted by (Pb)(CoW)TiO₃, while the adhesive is made of PZT-5, whose mechanical properties are shown in Table 1.

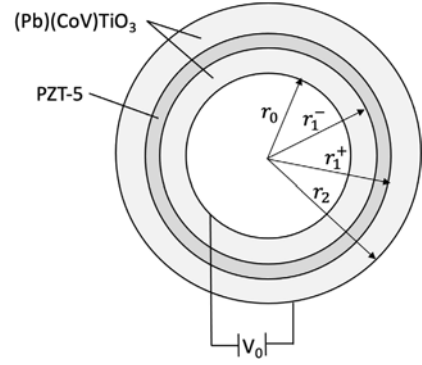


Fig. 2. Geometry of the three-layers hollow piezoelectric composite sphere.

Table 1
Piezoelectric material properties for (Pb)(CoW)TiO₃ and PZT-5.

Moduli	(Pb)(CoW)TiO ₃	PZT-5
c_{11} , GPa	128	111
c_{12} , GPa	32.3	32.2
c_{22} , GPa	150	120
c_{23} , GPa	37.1	75.2
e_{11} , C/m ²	8.5	15.78
e_{12} , C/m ²	1.61	-5.35
β_{11}/ϵ_0	209	1700

The piezoelectric hollow composite sphere is subjected to an electric potential $V_0 = 10$ V, applied on the inner surface, while the electric potential is set equal to zero on the outer boundary, so that $\phi(r_0) = V_0$ and $\phi(r_2) = 0$. Free mechanical boundary conditions on both internal and external surfaces are imposed, meaning that $\sigma_r(r_0) = 0$ and $\sigma_r(r_2) = 0$. In this case the sphere behaves as an actuator. Following the ideas proposed in [25], the numerical results for the variables are provided using the dimensionless units. For an applied electric potential V_0 , we set:

$$(U_r, \Phi) = \frac{E_0}{V_0} (u_r, \phi/E_0), \quad (\Sigma_r, D_r) = \frac{hE_0}{C_{00}V_0} (\sigma_r, E_0 D_r),$$

where, for numerical convenience, $E_0 = 10^9$ Vm⁻¹ and $C_{00} = 1$ GPa.

Let us consider the closed-form solution (18) for each of the three layers. By applying the aforementioned set of boundary conditions and continuity conditions at the interface between adherents and adhesive, the twelve unknown integration constants can be easily found. Hence, the analytical solution for a three-phases hollow piezoelectric sphere is completely determined in terms of U_r , Σ_r , Φ and D_r .

The exact solution is compared with the closed-form solution, analogously obtained for a two-phases hollow composite sphere, in which the intermediate layer is replaced by the generalized interface conditions (12) (see Section 2.3).

First, the influence of the relative thickness of the intermediate layer ϵ/h is investigated in order to evaluate the accuracy of the asymptotic modeling. In particular, the quality of the solution is evaluated considering the L²-relative error $\frac{\|s^\epsilon - s_{model}\|}{\|s^\epsilon\|}$, where s^ϵ denotes the reference solution computed using the three-phases problem, while s_{model} indicates the solution of the interface model. The convergence of the general interface model towards the three-phases one with respect to the thickness ratio ϵ/h is presented in Fig. 3.

From the plot, it can be observed that, by reducing the thickness of the adhesive, the relative error has a drastic reduction and so, the proposed general interface model provides an acceptable solution and it is able to correctly approximate the exact solution s^ϵ . For instance, when the relative thickness is 0.01, the relative error is closed to 1.147% and 2.146%, concerning the displacement and radial stress, respectively. The error significantly reduces to 0.0039% and 0.0064%, concerning

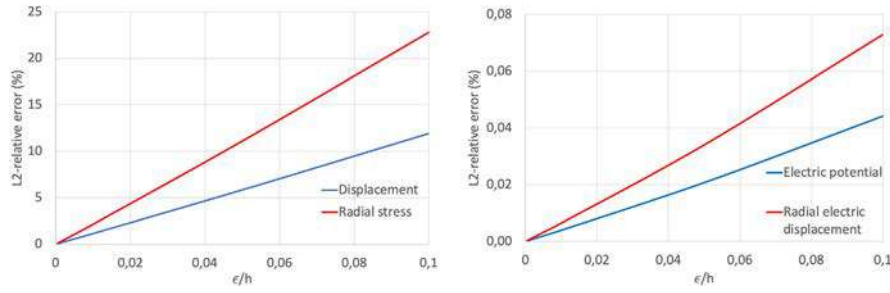


Fig. 3. Convergence diagram with respect to the relative thickness ϵ/h .

Table 2

L^2 -relative errors values.

ϵ/h	U_r error (%)	Σ_r error (%)	Φ error (%)	D_r error (%)
0.1	11.9278	22.7947	0.0442	0.0729
0.01	1.1471	2.1461	0.0039	0.0064
0.001	0.1142	1.0673	0.0004	0.0006

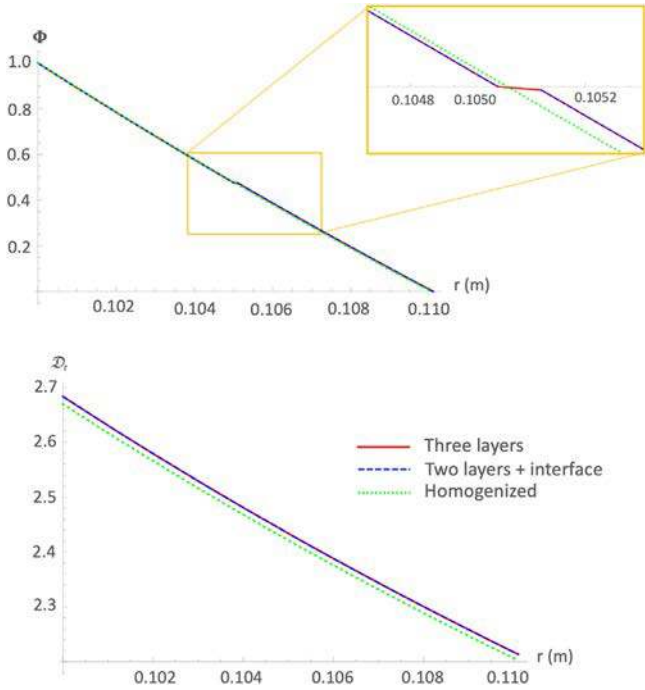


Fig. 4. Electric potential and electric displacement vs radius, $\epsilon/h = 0.01$ ϵ/h .

the electric potential and radial electric displacement, respectively. Table 2 reports the relative error values for vanishing relative thickness.

Figs. 4 and 5 show the trends of the electric potential, electric displacement, radial stress and radial displacement along the radial coordinate, for a fixed $\epsilon/h = 0.01$. The diagrams report the comparison among three closed-form solutions relative to the following configurations: (i) the three-layers composite sphere; (ii) the two-layers composite sphere with the general interface law; (iii) the single-layer sphere with homogenized coefficients, obtained by means of the transfer matrix method (see Section 3.3).

The diagrams confirm a very good agreement between the exact three-layers solution (red continuous curves) and the two-layers solution with interface conditions (blue dashed curves) in terms of electric potential, electric displacement and radial displacement. Concerning the radial stress, the overall trend is well-approximated, even though the jump at the interface is slightly overestimated by the

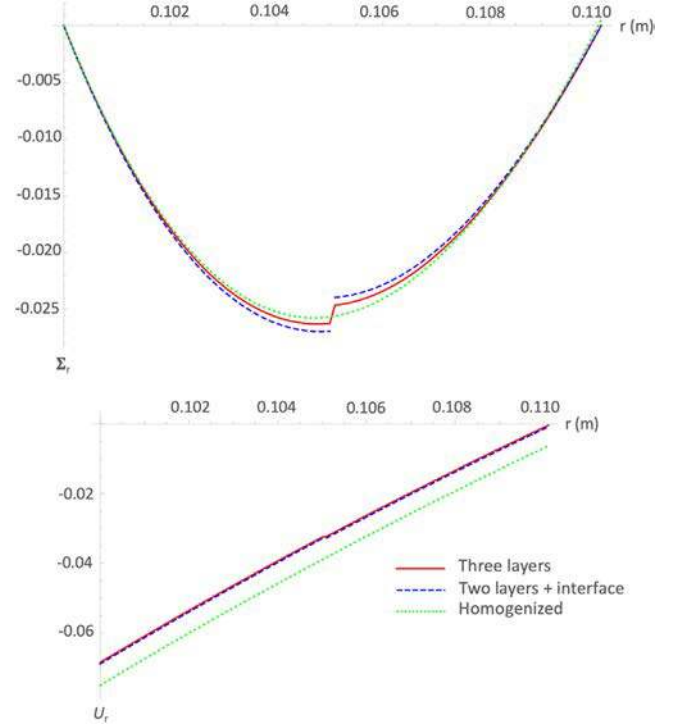


Fig. 5. Radial stress and displacement vs radius, $\epsilon/h = 0.01$.

two-layers + interface model. As expected, the homogenized solution, obtained through Bifulco's approach, manages to capture the global electromechanical behavior on the average. However, it appears to give moderately inaccurate estimates, concerning the electric and radial displacements values.

The transfer matrix method allows the evaluation of the equivalent radial and tangential Young's moduli and Poisson's coefficients for the spherical composite from Eqs. (23). Indeed, for this particular case, one has: $E = 1.4052 \times 10^{11}$ N/m², $E' = 1.4871 \times 10^{11}$ N/m², $\nu = 0.1933$ and $\nu' = 0.2047$.

5. Concluding remarks

A general imperfect interface model for piezoelectric hollow spherical composites has been proposed. The approach is based on the asymptotic expansions method, characterizing the order 0 and order 1 interface laws. Following [24], a general transmission law, comprising soft, hard and rigid interface conditions at the various order, has been derived. A generalization of the transfer matrix method [33] has been proposed for piezoelectric hollow spherical composites. In order to assess the validity of the previous asymptotic and homogenization procedures, the analytical solution of a piezoelectric hollow sphere

subjected to an applied electric potential has been developed, taking also into account the aforementioned general interface laws. The convergence results showed that, by reducing the thickness of the adhesive, the relative error has a drastic reduction. Moreover, the numerical result reported a very good agreement between the exact three-layers solution and the two-layers solution with interface conditions in terms of electric potential, electric displacement and radial displacement.

CRedit authorship contribution statement

M. Serpilli: Conceptualization, Methodology, Formal analysis, Investigation, Data curation, Writing – original draft, Writing – review & editing. **R. Rizzoni:** Conceptualization, Methodology, Writing – review & editing, Supervision. **S. Dumont:** Conceptualization, Methodology, Supervision. **F. Lebon:** Conceptualization, Methodology, Supervision.

Declaration of competing interest

The authors declare that they have no known competing financial interests or personal relationships that could have appeared to influence the work reported in this paper.

Appendix

The coefficients of the equilibrium and electrostatic problem solution for a piezoelectric hollow sphere are equivalent to those obtained in [7] and take the following expressions:

$$\begin{aligned}\gamma &:= c_{11} + \frac{e_{11}^2}{\beta_{11}} \\ \beta &:= \frac{1}{\gamma} \left(c_{22} + c_{23} - c_{12} + \frac{e_{12}}{\beta_{11}} (2e_{12} - e_{11}) \right) \\ a_{11} &:= c_{11}\alpha_1 + 2c_{12} + \alpha_1 e_{11} \left(\frac{e_{11}}{\beta_{11}} + \frac{2}{\alpha_1} \frac{e_{12}}{\beta_{11}} \right), \\ a_{12} &:= c_{11}\alpha_2 + 2c_{12} + \alpha_2 e_{11} \left(\frac{e_{11}}{\beta_{11}} + \frac{2}{\alpha_2} \frac{e_{12}}{\beta_{11}} \right), \\ a_{13} &:= (2c_{12} - c_{11}) \frac{e_{12}}{\beta\gamma\beta_{11}} - e_{11} \left(\frac{e_{12}(e_{11} - 2e_{12})}{\beta\gamma\beta_{11}^2} + \frac{1}{\beta_{11}} \right), \\ a_{23} &:= \frac{e_{12}}{\beta_{11}\beta\gamma}, \\ a_{41} &:= \frac{e_{11}}{\beta_{11}} + \frac{2}{\alpha_1} \frac{e_{12}}{\beta_{11}}, \\ a_{42} &:= \frac{e_{11}}{\beta_{11}} + \frac{2}{\alpha_2} \frac{e_{12}}{\beta_{11}}, \\ a_{43} &:= \frac{e_{12}(e_{11} - 2e_{12})}{\beta\gamma\beta_{11}^2} + \frac{1}{\beta_{11}}.\end{aligned}$$

References

- [1] Diab D, Lefebvre F, Nassar G, Smagin N, Isber S, Omar FEI, Naja A. An autonomous low-power management system for energy harvesting from a miniaturized spherical piezoelectric transducer. *Rev Sci Instrum* 2019;90:075004.
- [2] Sadeghpour S, Meyers S, Kruth JP, Vleugels J, Kraft M, Puers R. Resonating shell: A spherical-omnidirectional ultrasound transducer for underwater sensor networks. *Sensors* 2019;19:757.
- [3] Kong QZ, Fan SL, Bai XL, Mo YL, Song GB. A novel embeddable spherical smart aggregate for structural health monitoring: Part I. Fabrication and electrical characterization. *Smart Mater Struct* 2017;26:095050.
- [4] Li XF, Peng XL, Lee KY. The static response of functionally graded radially polarized piezoelectric spherical shells as sensors and actuators. *Smart Mater Struct* 2010;19:035010.

- [5] Singh VK, Singh J, Rao KVenkata, Singh NK, Saran C, Paswan M, Panda SK, Chaudhary V. Control of elastic behavior in smart material integrated shallow spherical composite panel using HOSDT kinematics. *Comput Struct* 2021;260:260113504, 26.
- [6] Ding HJ, Wang HM, Chen WQ. Analytical solution for the electroelastic dynamics of a nonhomogeneous spherically isotropic piezoelectric hollow sphere. *Arch Appl Mech* 2003;73:49–62.
- [7] Ghorbanpour A, Golabi S, Saadatfar M. Stress and electric potential fields in piezoelectric smart spheres. *J Mech Sci Technol (KSME Int J)* 2006;20(11):1920–33.
- [8] Ghorbanpour A, Kolahchi R, Mosallae Barzoki AA, Loghman A. Electro-thermo-mechanical behaviors of FGPM spheres using analytical method and ANSYS software. *Appl Math Model* 2012;36:139–57.
- [9] Chen WQ, Shioya T. Piezothermoelastic behavior of a pyroelectric spherical shell. *J Therm Stresses* 2001;24:105–20.
- [10] Saadatfar M, A Rastgoo. Stress in piezoelectric hollow sphere with thermal gradient. *J Mech Sci Technol* 2008;22:1460–7.
- [11] Arefi M, Khoshgoftar MJ. Comprehensive piezo-thermo-elastic analysis of a thick hollow spherical shell. *Smart Struct Syst* 2014;14:225–46.
- [12] Arefi M, Nahas I. Nonlinear electro thermo elastic analysis of a thick spherical functionally graded piezoelectric shell. *Comput Struct* 2014;118:510–8.
- [13] Atashipour SA, Sburlati R. Electro-elastic analysis of a coated spherical piezoceramic sensor. *Comput Struct* 2016;156:399–409.
- [14] Wang S, Shuyu L. A novelly universal theory: Toward accurately evaluating radial vibration characteristics for radially sandwiched spherical piezoelectric transducer. *Ultrasonics* 2021;111:106299.
- [15] Benveniste Y. The effective conductivity of composites with imperfect thermal contact at constituent interfaces. *Int J Eng Sci* 1986;24:1537–52.
- [16] Benveniste Y. Effective thermal-conductivity of composites with a thermal contact resistance between the constituents-nondilute case. *J Appl Phys* 1987;61:2840–3.
- [17] Javili A, Kaessmair S, Steinmann P. General imperfect interfaces. *Comput Methods Appl Mech Engrg* 2014;275:76–97.
- [18] Serpilli M, Lenci S. Asymptotic modelling of the linear dynamics of laminated beams int. *J Solids Struct* 2012;49(9):1147–57.
- [19] Serpilli M, Lenci S. An overview of different asymptotic models for anisotropic three-layer plates with soft adhesive. *Int J Solids Struct* 2016;81:130–40.
- [20] Lebon F, Rizzoni R. Asymptotic analysis of a thin interface: the case involving similar rigidity. *Internat J Engrg Sci* 2010;48:473–86.
- [21] Lebon F, Rizzoni R. Asymptotic behavior of a hard thin linear interphase: An energy approach. *Int J Solids Struct* 2011;48:441–9.
- [22] Rizzoni R, Dumont S, Lebon F, Sacco E. Higher order model for soft and hard elastic interfaces. *Int J Solids Struct* 2014;51:4137–48.
- [23] Dumont S, Rizzoni R, Lebon F, Sacco E. Soft and hard interface models for bonded elements. *Composites B* 2018;153:480–90.
- [24] Serpilli M, Rizzoni R, Lebon F, Dumont S. An asymptotic derivation of a general imperfect interface law for linear multiphysics composites. *Int J Solids Struct* 2019;180–181:97–107.
- [25] Dumont S, Serpilli M, Rizzoni R, Lebon F. Numerical validation of multiphysics imperfect interfaces models. *Front Mater* 2020;158:1–13. <http://dx.doi.org/10.3389/fmats.2020.00158>.
- [26] Serpilli M. On modeling interfaces in linear micropolar composites. *Math Mech Solids* 2018;23(4):667–85.
- [27] Serpilli M. Classical and higher order interface conditions in poroelasticity. *Ann Solid Struct Mech* 2019;11(1–2).
- [28] Serpilli M, Dumont S, Rizzoni R, Lebon F. Interface models in coupled thermoelasticity. *Technologies* 2021;9(1):17.
- [29] Serpilli M. Mathematical modeling of weak and strong piezoelectric interfaces. *J Elast* 2015;121(2):235–54.
- [30] Serpilli M. Asymptotic interface models in magneto-electro-thermo-elastic composites. *Meccanica* 2017;52(6):1407–24.
- [31] Guinovart-Sanjuán D, Rizzoni R, Rodríguez-Ramos R, Guinovart-Díaz R, Bravo-Castillero J, Alfonso-Rodríguez R, Lebon F, Dumont S, Sevostianov I, Sabina FJ. Behavior of laminated shell composite with imperfect contact between the layers. *Comput Struct* 2017;176:539–46.
- [32] Buefler H. Theory of elasticity of a multilayered medium. *J Elast* 1971;1(2):125–43.
- [33] Buefler H. The arbitrarily and the periodically laminated elastic hollow sphere: Exact solutions and homogenization. *Arch Appl Mech* 1998;68:579–88.
- [34] Molotkov LA. New method for deriving equations of an effective average model of periodic media. *J Soviet Math* 1992;62:3103–17.
- [35] Molotkov LA. On methods of deriving equations describing effective models of layered media. *J Math Sci (N Y)* 2000;102:4275–90.